Fuel 300 (2021) 120927

Contents lists available at ScienceDirect

Fuel

journal homepage: www.elsevier.com/locate/fuel

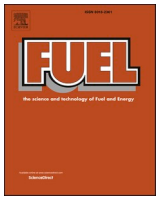

Full Length Article

# Catalytic hydrothermal carbonization of microalgae biomass for low-carbon emission power generation: the environmental impacts of hydrochar co-firing

Greta Sztancs [a], Attila Kovacs [b], Andras Jozsef Toth [a], Peter Mizsey [c], Pieter Billen [b], Daniel Fozer [a,*]

[a] Department of Chemical and Environmental Process Engineering, Budapest University of Technology and Economics, Budafoki út 8., 1111 Budapest, Hungary
[b] Department of Chemistry/Biochemistry, iPRACS, University of Antwerp, Antwerp, Belgium
[c] Department of Fine Chemicals and Environmental Technology, University of Miskolc, Egyetem út, 3515 Miskolc, Hungary

ARTICLE INFO

*Keywords:*
Catalytic hydrothermal carbonization
Hydrochar
Biofuel
Co-firing
GHG footprint
Life cycle assessment

ABSTRACT

This work aims to improve the synthesis of renewable hydrochar (HC) co-fired with coal to reduce grenhouse gas (GHG) emission. Acetic acid catalyzed hydrothermal carbonization (cHTC) of *Chlorella vulgaris* microalgae biomass was investigated based on a $3^{3-1}$ fractional statistical design of the experiment to examine the effects of hydrothermal reaction temperature (T = 180–220 °C), biomass-to-suspension- (BSR = 5–25 wt.%), and catalyst-to-suspension (CSR = 0–10 wt.%) ratios on process performance indicators. Analysis of variance was used to assess the experimental data. The results show that the application of homogeneous catalyst improves the fuel ratio and energy recovery efficiency up to 0.38 and 36.3%. *Ex-ante* cradle-to-gate life cycle assessment was performed to evaluate the impacts of co-firing ratio (CFR) and hydrochar quality on multi-perspective mid-, and endpoint environmental indicators. The highest decarbonization potential (−1.54 kg $CO_{2,eq}$ $kWh^{-1}$) is achieved using catalytic hydrochar biofuel produced at 195 °C, 25 wt.% BSR, and 8 wt.% CSR levels. The application of catalytic and autocatalytic hydrochar blends improves the overall environmental impacts and greenhouse gas footprint of solid fuel firing facilitating the transition toward low-carbon emission power generation.

## 1. Introduction

The fast-growing population, increasing global energy needs and climate change call for effective carbon dioxide removal (CDR) technologies that can contribute to shift energy production toward carbon neutrality [1]. Bioenergy with carbon capture and utilization (BECCU) offers a large-scale exploitable solution to (1) neutralize anthropogenic $CO_2$, (2) transform it into low-carbon synthetic fuels and materials and (3) to strengthen energy security [2].

Microalgae biomass are promising BECCU organisms characterized by high biodiversity, robust photosynthetic activity (with an approximate solar energy conversion efficiency of 9–10% [3]), and biomass productivity [4]. Microalgae can be cultivated in closed photobioreactors and open raceway-pond systems with high $CO_2$ biofixation rate, however, the downstream processing of cells is limited because of the dilute suspensions derived from the fermentation phase [5]. Conventional thermochemical conversion technologies (e.g., torrefaction, pyrolysis) require the prior drying of the wet biomass, decreasing the overall process efficiency and increasing operational costs. To overcome this bottleneck hydrothermal – high pressure and temperature – technologies [6] can be applied utilizing the excess water content of the feedstock as a reagent and solvent at the same time and increasing the energy conversion efficiency [7].

In terms of air pollution and attributed climate hazards, there is an urging demand for replacing coal-fired plants with renewable energy [8,9]. The transition towards climate-neutrality requires a variety of steps on different fronts, including the altering of existing fossil energy infrastructure. Coal blending is a frequently used technique to improve energy decentralization, environmental and technical properties of solid fuel firing. Major blending types include *(i)* coal-coal [10], *(ii)* coal-biomass [11] and *(iii)* coal-opportunity fuel [12] mixtures. The coal-coal blending is often used to reduce sulfur content, control the amount of inorganic constituents and moderate the reactivity of the total supply of fossil fuel. However, this latter type of blending does not mitigate the environmental effects of fossil fuels. Biomass co-firing has

* Corresponding author.
*E-mail address:* daniel.fozer@edu.bme.hu (D. Fozer).

https://doi.org/10.1016/j.fuel.2021.120927
Received 31 January 2021; Received in revised form 13 April 2021; Accepted 21 April 2021

**Nomenclature**

| | |
|---|---|
| ANOVA | Analysis of variance |
| ASTM | American Society for Testing Materials |
| BECCU | Bioenergy with carbon capture and utilization |
| BSR | Biomass-to-suspension ratio (wt.%) |
| c | Latent heat of vaporization (MJ $kg^{-1}$) |
| CC | Carbon content (wt.%) |
| CDR | Carbon dioxide removal |
| CFR | Co-Firing Ratio (%) |
| CFPP | Coal-Fired Power Plant |
| CHC | Carbohydrate content (wt.%) |
| CHP | Combined Heat and Power |
| cHTC | Catalytic hydrothermal carbonization |
| cHTP | Carcinogenic human toxicity potential |
| $c_p$ | Specific heat (MJ $kg^{-1}$ $K^{-1}$) |
| Cv | *Chlorella vulgaris* |
| $c_w$ | Heat of evaporation of water (MJ $kg^{-1}$) |
| CSR | Catalyst-to-suspension ratio (wt.%) |
| df | Degree of freedom (–) |
| DW | Dry weight (kg) |
| ED | Energy densification (–) |
| F | Fischer's variance ratio (–) |
| FC | Fixed carbon (wt.%) |
| FR | Fuel ratio (–) |
| GHG | Greenhouse gas |
| GWP | Global warming potential (kg $CO_{2,eq}$) |
| HC | Hydrochar |
| HCo | Hard coal |
| HHV | Higher heating value (MJ $kg^{-1}$) |
| HTC | Hydrothermal carbonization |
| HTG | Hydrothermal gasification |
| HTL | Hydrothermal liquefaction |
| L | Linear |
| LC | Lipid content (wt.%) |
| LCA | Life cycle assessment |
| LCI | Life cycle inventory |
| m | Mass (kg) |
| MA | Microalgae |
| NER | Net energy ratio (–) |
| PC | Protein content (wt.%) |
| PM | Particulate matter |
| PW | Process water |
| Q | Quadratic |
| $Q_{input}$ | Input energy (MJ) |
| $Q_{output}$ | Output energy (MJ) |
| $R_{wind}$ | Share of wind energy in the applied energy mix (%) |
| SS | Sum of squares |
| T | Temperature (°C) |
| TOC | Total organic carbon (mg $L^{-1}$) |
| VM | Volatile matter (wt.%) |
| W | Water |
| $X_{CFR}$ | Solid fuel-to-power efficiency (–) |
| $Y_{BC}$ | Biogas yield (mol $kg^{-1}$) |
| $Y_{HC}$ | Hydrochar yield (%) |
| $\eta_E$ | Electric efficiency (–) |
| $\eta_{ER}$ | Energy recovery efficiency (–) |
| $\eta_{FCR}$ | Fixed carbon recovery efficiency (–) |

more advantages over coal-coal firing since bio-based blends are abundant and renewable, the geographical energy decentralization can be improved and it opens an opportunity to reduce the greenhouse gas (GHG) emission of conventional processes [13]. On the other hand, the key challenges that arise during the utilization of biomass are: the (1) high moisture content of raw materials, (2) low energy density, (3) high volatile matter content, (4) presence of contaminants and heterogeneity (5) poor grindability, stability and hydrophilic behaviour [14]. Biochar has gained high attention as a renewable blending material because it enhances combustion quality [15] and the mitigation of attributed environmental impacts [16]. Yang et al. [17] investigated biomass co-firing plants and found that near zero emission can be achieved with 25% biomass co-firing if the plant structure involves carbon capture and storage units following the combustion process. Zhang et al. [18] studied hydrochar (HC) - anthracite co-combustion and found that HC can improve the combustion performance by decreasing the activation energy of combustion reactions. Sztancs et al. [19] showed that hydrochars are suitable blending components in co–hydrothermal gasification process to increase biogas yield and carbon conversion ratio.

Hydrothermal carbonization (HTC) is a promising thermochemical method enabling the transformation of high moisture containing feedstocks into solid biofuels (a.k.a., hydrochar) at mild subcritical reaction condition (180–250 °C, <100 bar) [20]. Huang et al. [21] showed that the hydrothermal carbonization of biomass can improve fuel properties by densifying the energy content of the feedstock and increasing its hydrophobicity and grindability. Studies focusing on noncatalytic hydrothermal conversion examined the role of independent process variables (e.g., temperature, pressure, biomass-to-suspension ratio, residence time, heating rate, pH) on product yields and characteristics in the cases of lignocellulosic [22], coniferous biomass [23], sewage sludge [24] and also microalgae feedstocks (e.g., *Chlorella vulgaris* [25] and *Spirulina platensis* [26]). Temperature and pressure proved to be important parameters influencing the physical properties of water solvent and the fragmentation of biomass bonds [27]. It was expressed that the biomass-to-suspension ratio (BSR) could intensify the hydrolysis at lower factor levels raising the calorific value but reducing achievable hydrochar yield [28].

The pH of the reaction medium decreases during the sub-critical hydrothermal conversion as a result of *in situ* acid formation (e.g., formic acid, acetic acid, lactic acid and levulinic acid) [29]. The acidic compounds act as autocatalysts advancing the decomposition of biomacromolecules, the hydrolysis, decarboxylation and the formation of HCs [30]. Additionally, the increased concentration of $H^+$and $OH^-$ and ionic strength advance thermochemical reaction rates [31]. The utilization of acid (HCl, $CH_3COOH$) or alkali catalysts (NaOH, KOH, $Na_2CO_3$, $K_2CO_3$) can also improve product quality (e.g., pore structure, adsorptive capacity, specific surface area) [32].

The application of renewable biofuels as blending components is a promising way to decrease the negative environmental effects of conventional energy vectors in the short run, and beneficially use existing infrastructure to do so. Benavente et al. [33] performed life cycle assessment (LCA) to compare the environmental impacts - including global warming potential (GWP), human toxicity, terrestrial, freshwater and marine eutrophication - of olive mill waste upgrading via biological and thermochemical processes (including hydrothermal carbonization, aerobic composting, anaerobic digestion and incineration). It was found that low-carbon operation could be achieved by applying hydrothermal conversion and combustion of hydrochar solid fuels. However, HC production had high impact on freshwater eutrophication and freshwater ecotoxicity due to the formation of process water (PW). Tradler et al. [34] found that the total organic carbon concentration of PW can be decreased by 90% applying UV radiation treatment in order to comply with existing regulations. It was highlighted that PW contains acidic compounds that could be recirculated to the HTC process as

catalysts. Process water also contains biogenic elements that could be reused in the microalgae cultivation to decrease additional micronutrients demands [35]. Owsianiak et al. [36] examined the environmental impacts of the hydrothermal carbonization process with four different feedstock raw materials: green waste, food waste, organic fraction of municipal solid waste and digestate. It was determined that replacing hard coal briquettes with hydrochars derived from green waste associated with a cumulated −0.54 kg $CO_{2,eq}$ $kg^{-1}$ emission rate. Reimann et al. [37] found that the global warming potential of hydrothermal carbonization is lower compared to conventional technologies when the raw materials are part of the biogenic cycle (e.g., biomass residues) but stated the need for complex life cycle evaluations regarding hydrothermal processes.

In the present study, the (*i*) hydrothermal valorization of microalgae biomass, (*ii*) greenhouse gas footprints of catalytic hydrothermal carbonization and (*iii*) the environmental impacts of solid fuel co-firing are investigated. Thermocatalytic measurements were carried out based on a fractional factorial design of the experiment and evaluated using analysis of variance in order to (1) determine the effects of reaction parameters on process performance indicators, to (2) supply missing data for early-stage multi-perspective life cycle assessment and to (3) assist in making the trade-off between achievable combustion quality and product yield based on environmental criteria. The acetic acid catalyzed hydrothermal conversion of aquatic microalgae biomass is found to be a beneficial valorization technique for the production of high quality renewable solid blending components. The synthesized hydrochars are characterized by higher stability and energy density compared to raw biomass indicating effective fossil fuel substitution potentials. The best acetic acid catalyzed HTC experimental setup and hydrochar co-firing ratio (CFR) are determined enabling significant GHG footprint mitigation via co-combustion applications. The cradle-to-gate environmental damage assessment of co-firing shows that the utilization of catalytic and noncatalytic hydrochar blends contribute to decrease the climate change potential of conventional power generation.

## 2. Materials and methods

### 2.1. Materials

*Chlorella vulgaris* (*Cv*) microalgae strain was used during the experimental phase. The feedstock was purchased from commercial market in dried form. The proximate and ultimate analyses of *Cv* are presented in Table 3. Acetic acid (99.7%) was purchased from Sigma–Aldrich.

### 2.2. Hydrothermal carbonization

The thermochemical conversion was performed in a 250 mL non-stirred pressure vessel (Parr Instrument Company, MT-07300). The reactor was insulated with a rockwool cage and heated by a magnetic stirring hotplate (Heidolph MR 3003 control) with an average heating rate of 4.6 °C $min^{-1}$. 45 min residence time and autogenous pressure were applied for each experiment. Following the cHTC process, the co-produced biogas was gathered in a calibrated gas burette. The process water and the hydrochar were separated with a Hettich Rotina 380 1701 centrifuge at 5000 rpm for 20 min. The solid product was dried in a drying cabinet at 105 °C for constant weight.

### 2.3. Product analysis

#### 2.3.1. Proximate analysis

The proximate analysis of *Cv* and HC samples were performed according to the related standards of American Society for Testing Materials (ASTM). The volatile matter (VM, wt.%, Eq. 1) content was determined by igniting 1 g of microalgae or dry HC powder at 950 °C for 7 min (ASTM D3175). The ash content (wt.%, Eq. 2) of *Cv* was determined by heating 0.5 g of microalgae powder to 250 °C, igniting the sample at this temperature level for 30 min, then heating the furnace to 575 °C and igniting it for 3 h (ASTM E1755). The ash content of HCs was determined by heating the samples to 750 °C in 2 h then igniting them for 2 h (ASTM D3174). The measurements were carried out in a DENKAL 1.4/1000 electric furnace. Fixed carbon (FC, wt.%) content was calculated based on Eq. (3) according to ASTM D3172:

$$VM\left(wt.\%\right) = \frac{m_{initial} - m_{residual}}{m_{initial}} \cdot 100, \tag{1}$$

$$ash\left(wt.\%\right) = \frac{m_{residual}}{m_{initial}} \cdot 100, \tag{2}$$

$$FC\,(wt.\%) = 100 - VM - ash, \tag{3}$$

where $m_{initial}$ is the mass of dry *Cv* and HC samples before the ignition (g) and $m_{residual}$ is the mass of *Cv* and hydrochar samples following the ignition (g).

#### 2.3.2. Biogas analysis

The composition of HTC biogas was analyzed using a HP5890SII/TCD/FID gas chromatography system equipped with a 1.9 m length, 1/8" OD packed stainless steel column filled with 80/100 mesh Porapak Q load. The initial temperature of the oven was set to 50 °C and this temperature was held for 30 s. The temperature was increased by 20 °C $min^{-1}$ to a final temperature of 150 °C, which was held for 2 min. Argon was selected as carrier gas with an inlet column head pressure of 150 kPa.

#### 2.3.3. Process water analysis

The total organic carbon (TOC) content and the pH of the co-product PW were measured using a Shimadzu TOC-VCSN analyzer and Oakton pH 100 meter.

### 2.4. Experimental design and statistical analysis

STATISTICA v13.4 software [38] was used for statistical and graphical evaluations. A $3^{3-1}$ fractional factorial design of the experiment was employed to investigate the cHTC process. The independent variables were (1) biomass-to-suspension ratio, (2) catalyst-to-suspension ratio and (3) temperature with factor levels ranging between 5–25 wt.%, 0–10 wt.% and 180–220 °C. The dependent variables were VM, ash, FC contents of HC, HC yield ($Y_{HC}$) and total organic carbon content of process water. The 5 dependent variables were evaluated using Analysis of Variance (ANOVA). The applied polynomial quadratic response model was given by Eq. (4):

$$\widehat{Y}_i = b_0 + \sum_{i=1}^{k} b_i x_i + \sum_{i=1}^{k} b_{ii} x_i^2 + \epsilon, \tag{4}$$

where $\widehat{Y}_i$ is the predicted response variable, $x_i$is the value of independent variables, $b_0, b_i$and $b_{ii}$are the regression coefficients and $\epsilon$ is the random error.

### 2.5. Calculations

#### 2.5.1. HC quality and HTC conversion efficiency

The hydrochar yield was determined using Eq. (5):

$$Y_{HC}\left(\%\right) = \frac{m_{HC}}{m_{MA}} \cdot 100, \tag{5}$$

where $m_{HC}$is the mass of hydrochar (kg) and $m_{MA}$is the mass of dry microalgae (kg).

The quality of the produced HC and the efficiency of the hydrothermal conversion were evaluated by the higher heating value [39]

(Eq. (6)), fuel ratio (FR) (Eq. (7)), energy densification (ED) (Eq. (8)), energy recovery-, ($\eta_{ER}$) (Eq. (9)) and fixed carbon recovery efficiencies ($\eta_{FCR}$) (Eq. 10):

$$HHV\left(MJ\ kg^{-1}\right) = 0.3536{\cdot}FC + 0.1559{\cdot}VM - 0.0078{\cdot}ash \tag{6}$$

$$FR\ \left(-\right) = \frac{FC}{VM} \tag{7}$$

$$ED\ \left(-\right) = \frac{HHV_{HC}}{HHV_{MA}} \tag{8}$$

$$\eta_{ER}\ \left(-\right) = \frac{HHV_{HC}}{HHV_{MA}}{\cdot}Y_{HC} \tag{9}$$

$$\eta_{FCR}\ \left(-\right) = \frac{FC_{HC}}{FC_{MA}}{\cdot}Y_{HC} \tag{10}$$

The HHV's empirical formula is applicable in a wide range of VM (0.9%–90.6%), ash (0.2–77.7%) and FC contents (1.0%–91.5%) where the average absolute and bias errors are 3.74% and 0.12%, respectively. The stability and ignition characteristics of HC samples were assessed by the fuel ratio. Leng et al. [40] expressed that a FR value higher than 1.14 predicts stable char with a half-life of minimum 1000 years. A FC/VM ratio between 0.33 and 1.14 indicates moderately stable fuel with a half-life of 100–1000 years, while a fuel ratio lower than 0.33 denotes non-stable char with a half-life of maximum 100 years. Higher FR values are desired to increase stability of solid fuels but the ratio should be below 2.5 to ensure satisfactory VM content, fuel reactivity and combustion performance [41].

### 2.5.2. Energy efficiency of cHTC process

The energy consumption (Eq. (11)), rate of energy recovery (Eq. (12)) and net energy ratio (NER) (Eq. (13)) of catalytic and non-catalytic hydrothermal carbonizations were calculated as follow:

$$Q_{IN,HTC}\ \left(MJ\right) = \sum m_k{\cdot}c_{p,k}{\cdot}\triangle T_{HTC} + Q_c + m_{w,HC}{\cdot}\left(c_W + c_{p,W}{\cdot}\triangle T_{drying}\right), \tag{11}$$

$$Q_{OUT,HTC}\ \left(MJ\right) = m_{HC}{\cdot}HHV_{HC}, \tag{12}$$

$$NER_{HTC}\ \left(-\right) = \frac{Q_{OUT,HTC}}{Q_{IN,HTC}}, \tag{13}$$

where $Q_{IN,HTC}$ is the input energy requirement of hydrothermal carbonization (MJ), $Q_{OUT,HTC}$is the output energy gain via the hydrothermal conversion (MJ), $m_k$ is the mass of the kthcompound (kg) where k equals to water, microalgae and acetic acid. $c_{p,k}$ is the specific heat of the kthcompound (MJ $kg^{-1}K^{-1}$), $m_W$ is the mass of water (kg), $c_w$ is the heat of evaporation of water (MJ $kg^{-1}$), $c_{p,W}$ is the specific heat of water (MJ $kg^{-1}K^{-1}$), $\triangle T_{HTC}$is the temperature difference between room temperature and HTC reaction temperatures (K). $Q_c$ is the energy consumption of centrifugation ($2.17 \cdot 10^{-2}$kWh $kg^{-1}$(dry weight) [42]), $m_{w,HC}$ is the mass of the residual moisture content of dewatered hydrochar (kg), $\triangle T_{drying}$is the temperature difference between room temperature and drying temperature (105 °C), $m_{HC}$ is the mass of hydrochar (kg) and $HHV_{HC}$is the higher heating value of hydrochar (MJ $kg^{-1}$).

The specific heat of microalgae was determined based on its lipid ($LC_{MA}$), protein ($PC_{MA}$), and carbohydrate ($CHC_{MA}$) contents (wt.%) using Eqs. (14)–(17) [43]:

$$c_{p,MA}\ \left(MJ\ kg^{-1}K^{-1}\right) = LC_{MA}{\cdot}c_{p,\ L} + PC_{MA}{\cdot}c_{p,P} + CHC_{MA}{\cdot}c_{p,CH}, \tag{14}$$

$$c_{p,L}\ \left(MJ\ kg^{-1}\ K^{-1}\right) = 0.40{\cdot}c_{p,W}, \tag{15}$$

$$c_{p,P}\ \left(MJ\ kg^{-1}\ K^{-1}\right) = 0.37{\cdot}c_{p,\ W}, \tag{16}$$

$$c_{p,CH}\ \left(MJ\ kg^{-1}\ K^{-1}\right) = 0.34{\cdot}c_{p,W}, \tag{17}$$

where $c_{p,L}$, $c_{p,P}$and $c_{p,CH}$are the specific heats of lipid, protein and carbohydrate (MJ $kg^{-1}K^{-1}$), respectively. It is assumed that the used *Chlorella vulgaris* feedstock contains 40 wt.% lipid, 48 wt.% protein and 12 wt.% carbohydrate.

### 2.5.3. Electric efficiency of HC and HCo co-firing

Combined heat and power (CHP) plant configuration was considered for solid fuel co-firing. It was estimated that 25% of input energy is lost during the combustion process. The heat and electricity generation efficiencies were assumed to be 45% and 30%, respectively [44]. The feedstock-to–hydrochar-to-power efficiency ($\eta_{E,HC}$) was calculated based on Eq. (18):

$$\eta_{E,HC}\ \left(-\right) = \frac{Q_{OUT,HTC}}{\sum E_{IN,k}}{\cdot}\frac{\theta_{CHP,e}}{100}, \tag{18}$$

where $Q_{OUT,HTC}$is the energy stored in hydrochar carrier (MJ), $\theta_{CHP,e}$is the estimated electricity producing efficiency of the CHP plant (30%) and $\sum E_{IN,k}$is the sum of the required input energy (MJ). $\sum E_{IN,k}$ consists of the energy needs of (1) chemicals production (i.e., fertilizers, flocculant, homogeneous catalyst), (2) microalgae cultivation, (3) *Chlorella vulgaris* harvesting and dewatering, (4) raw material mixing, (5) hydrothermal carbonization and (6) HC dewatering. The overall electricity conversion efficiency of solid fuel co-firing was determined based on Eq. 19:

$$X_{CFR}\ \left(-\right) = \frac{m_{HC}}{m_{HC} + m_{HCo}}{\cdot}\eta_{E,HC} + \frac{m_{HCo}}{m_{HC} + m_{HCo}}{\cdot}\eta_{E,HCo}, \tag{19}$$

where $X_{CFR}$is the feedstock-to-power co-firing efficiency (–), $m_{HCo}$is the mass of hard coal (kg). The hard coal electricity conversion efficiency ($\eta_{E,HCo}$) was estimated to be 0.367 [45].

### 2.5.4. Technology overview

*2.5.4.1. Microalgae cultivation.* The life cycle inventory inputs of microalgae cultivation were substrates (carbon dioxide, nutrients (N and P sources), light) and utilities. Outdoor open raceway ponds were considered for the cultivation stage. It was assumed that at the end of the fermentations the dry weight content of culture broth reaches 0.5 g $L^{-1}$ [46]. The $CO_2$ uptake during the biofixation was determined by Eq. 20 assuming that the $CO_2$ is sequestrated from the atmosphere [47]:

$$m_{CO_2}\ \left(kg\right) = \frac{M_{CO_2}{\cdot}CC_{MA}}{M_C{\cdot}100}{\cdot}m_{MA}, \tag{20}$$

where $M_{CO_2}$ and $M_C$ are the molar weights of $CO_2$ and carbon (g $mol^{-1}$), $CC_{MA}$is the carbon content of microalgae (wt.%). Urea and diammonium phosphate (DAP) were considered as nitrogen and phosphorus sources. The required amount of N and P were calculated based on the Redfields molar ratio of marine phytoplanktons ($C_\alpha N_\beta P_\gamma$:$C_{106}N_{16}P_1$) by Eqs. (21)–(22) [48]:

$$m_N\ \left(kg\right) = \frac{\beta{\cdot}M_N{\cdot}\frac{CC_{MA}}{100}}{\alpha{\cdot}M_C}{\cdot}m_{MA}, \tag{21}$$

$$m_P\ \left(kg\right) = \frac{\gamma{\cdot}M_P{\cdot}\frac{CC_{MA}}{100}}{\alpha{\cdot}M_C}{\cdot}m_{MA}, \tag{22}$$

where $\alpha, \beta$ and $\gamma$ are the stoichiometric factors of C, N and P content of biomass feedstock (–), $CC_{MA}$ is the carbon content of microalgae (wt.%), $m_{MA}$ is the mass of microalgae (kg). $CC_{MA}$ was determined by Eq. (23)

[49]:

$$CC_{MA}\ (wt.\%) = 0.637 \cdot FC + 0.455 \cdot VM \quad (23)$$

The energy requirements of urea and DAP production were considered to be 26.12 MJ $kg^{-1}$and 14.47 MJ $kg^{-1}$ [50].

Taking into account geographical restrictions, it was assumed that solar energy is an adequate light source for the cultivation process. The circulation in the ponds was provided by paddlewheels to avoid sedimentation and self-shading. The area of raceway ponds was considered to be 5,000 $m^2$with an average biomass productivity of 15 g $m^{-2}d^{-1}$ [51], and paddlewheel energy requirement of 2,852 W $pond^{-1}$ [52].

*2.5.4.2. Harvesting and dewatering.* Following the upstream section, flocculation and sedimentation were considered for primary concentration of algae cells. Inorganic chemical flocculation was selected for this task due to the high obtainable harvesting efficiency (82.27%) [53] and low optimal dosage requirement of $Al_2(SO_4)_3$ flocculant (20 mg $L^{-1}$at pH 5) [54]. Lamella clarifiers were used for sedimentation with an estimated energy consumption of $3.91 \cdot 10^{-4}$kWh (kg algae DW)$^{-1}$. Following the primary dewatering step, the biomass concentration was considered to be as high as 30 g $L^{-1}$ [42].

Filtration was applied as a secondary concentration method. Netzsch chamber type pressure filtration was applied to achieve a final dry weight of 270 g $L^{-1}$. The energy consumption of a Netzsch chamber filter was 0.88 kWh $m^{-3}$ [55].

*2.5.4.3. Hydrothermal carbonization of biomass.* A static mixer was considered for the homogenization of microalgae feedstock and acetic acid catalyst with an estimated energy consumption of 10 kWh $m^{-3}$ [56]. Based on our measurements it is estimated that the residual moisture content of hydrochar is approximately 9 wt.% following the removal of the liquid co-product.

### 2.6. Life cycle assessment of HTC process

*Ex-ante* cradle-to-gate environmental assessment was performed based on ISO-14040 and ISO-14044 standards to determine the environmental impacts of the production and utilization of hydrochar blends and co-firing with hard coal. The LCAs were performed using SimaPro 9.1.1.1 software [57].

#### 2.6.1. Goal & Scope

The aims of the LCAs were (1) the evaluation of environmental impacts related to the application of hydrothermal carbonization, (2) the identification of environmental bottlenecks and (3) the determination of solid fuel co-firing ratios that enable GHG emission reduction. According to these objectives, nine LCA cases with different CFRs were considered and investigated as it is summarized in Table 1. The functional unit was 1 kWh of generated electricity. The system boundary for the environmental screening is illustrated in Fig. 1.

#### 2.6.2. Life cycle inventory (LCI)

The LCA inputs and outputs were compiled based on (1) cHTC and HTC experimental data, (2) calculations, (3) Ecoinvent v3.4 database [58] and (4) literature data. The life cycle inventory is summarized in Table 2. It is assumed that the input energy and utilities were provided by wind turbines and photovoltaic panels for hydrochar production stages. In the case of hard coal, the Ecoinvent v3.4 database was used to assess all of the inputs and outputs of high voltage electricity production. Freight trains were considered for the transportation of biomass and hard coal to an estimated distance of 100 km.

**Table 1**
Cases of life cycle assessment based on hydrochar and hard coal co-firing ratio (CFR).

| CFR (HC% in HC–HCo mix) | ID of the cases | |
|---|---|---|
| | cHTC process | HTC process |
| 100% | A1 | B1 |
| 75% | A2 | B2 |
| 50% | A3 | B3 |
| 25% | A4 | B4 |
| 0% | C | |

#### 2.6.3. Life cycle impact assessment

IMPACT2002 + v2.14 multi-perspective life cycle impact assessment (LCIA) method was used for the evaluation of GHG footprint (kg $CO_{2,eq}$$kWh^{-1}$) pollution indicator and damage categories such as human health ($\mu$Pt), ecosystem quality ($\mu$Pt), climate change ($\mu$Pt) and resources ($\mu$Pt). Monte Carlo simulations with 10,000 runs were carried out to investigate the uncertainty of input and output data. 95% confidence interval was applied during the uncertainty analysis.

## 3. Results

### 3.1. Production of hydrochar via catalytic hydrothermal carbonization

Acid catalyzed cHTC experiments were carried out in order (1) to investigate the effects of reaction parameters on the solid biofuel yield and quality, (2) to determine mathematical relationship between dependent and independent variables, (3) to improve the fuel properties and stability of hydrochar blends and (4) to provide missing input and output data for life cycle inventory. The experimental and calculated results of catalytic hydrothermal carbonization are presented in Table 3.

#### 3.1.1. Adequacy of statistical models

The ANOVA output tables of quadratic statistical models are given in Tables S1-S5. The statistical models and the regression coefficients are summarized in Table S6. High model accuracy was obtained in all cases (with R squared values higher than 0.95) indicating that regressions fit the measured data well. Fig. S1 shows that the predicted and observed values are close to each other confirming high model accuracy. The residues show normal distribution for each case (Fig. S2). Plotting predicted values in function of raw residuals do not show unique patterns affirming the adequacies of models (Fig. S3). The repeated control experiments are obtained within the ±95% confidence interval where the predicted and measured values are close to each other (as it is detailed in Table S7 and Fig. S4).

#### 3.1.2. The effects of process parameters on HTC performance

The analysis of variance results indicate that reaction temperature influences significantly the HC yield (T(L): F = 32.56, p = 0.029), volatile matter content (T(L): F = 129.82, p = 0.008; T(Q): F = 22.42, p = 0.042) and has a moderate effect ($0.05 < p < 0.10$) on the fixed carbon content (T(L): F = 37.74, p = 0.073; T(Q): F = 31.48, p = 0.085). Fig. 2a illustrates that lower temperature levels are preferred conditions to increase the hydrochar yield in the case of acid catalyzed hydrothermal conversion. This temperature dependent tendency is similar to the noncatalytic hydrothermal carbonization of wet biomass [60] but the rate of biofuel yield increment is higher than expected. The highest solid biofuel production rate ($Y_{HC}$=48.8%) is achieved at 180 °C, 25 wt.% BSR using 10 wt.% acetic acid catalyst-to-suspension ratio.

It is found that the temperature factor has also an important role in controlling the hydrochar's composition and indirectly fuel properties. Fig. 2b demonstrates that increased temperature levels are preferred to improve the fixed carbon content of the solid combustible samples. Analogous relationship is obtained in the case of noncatalytic hydrothermal conversion, i.e., raising the temperature from 180 °C to 220 °C results in a FC increment of 50.7% while the volatile matter content decreases by 7.2 wt.% using 15 wt.% biomass-to-suspension ratio. The rate of VM loss is higher than the growth of FC which indicates that volatile compounds are converted into liquid and gaseous substances

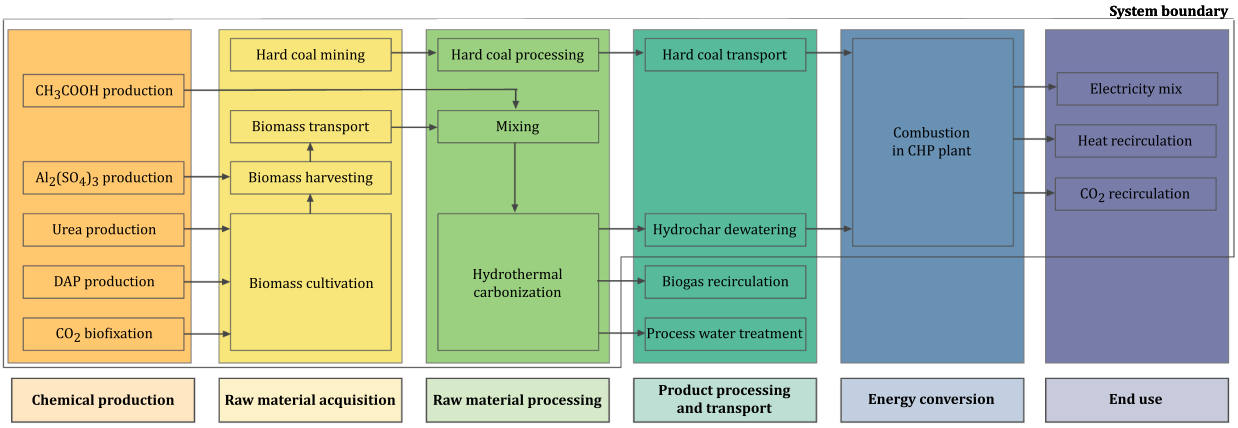


**Fig. 1.** Life cycle process inputs, outputs and system boundary of hydrochar and hard coal co-firing.

during the HTC process. Fig. 2c shows an inverse impact on the VM content, where increasing temperature levels have negative effects on the amount of volatiles. Lower VM and higher FC contents denote higher fuel ratio and better combustion characteristics. It is obtained that the fuel ratio can be increased up to 0.38 and 0.34 using 220 °C, 5 wt.% BSR factor levels and 9 & 5 wt.% CSR settings, respectively (as it is shown in Table S7). The solid renewable acid catalyzed HTC char products (1) have the same quality as sub-bituminous coals (19.30 MJ $kg^{-1}$<HHV <22.09 MJ $kg^{-1}$) according to the ASTM D388-13 standard, (2) are stable with a half-life of 100–1000 years frame (0.33 < FR < 1.14) and (3) have a satisfactory combustion performance (FR<2.5). On the other hand, improved combustion properties are coupled with lower solid biofuel yield highlighting the importance of the evaluation of the net energy ratio in function of catalytic and noncatalytic HTC experimental conditions.

The biomass-to-suspension ratio is obtained to be a significant factor regarding hydrochar's volatile matter (BSR (L): F = 35.35, p = 0.027; BSR (Q): F = 22.69, p = 0.041) and ash (BSR (L): F = 21.62, p = 0.043) contents. BSR has also a significant effect on the total organic carbon content (BSR (L):129.88, p = 0.007) of process water. The TOC content of process water samples is increasing at elevated biomass-to-suspension ratio levels as it is illustrated in Fig. 2d. Thus, it would be preferable to operate the thermochemical conversion at lower BSR factor levels to mitigate the formation of organic liquid compounds. On the other hand, higher biomass-to-suspension ratio levels contribute to achieve increased HC yield (BSR (L): F = 10.36, p = 0.084) (Fig. 2a). In the case of the noncatalyzed process the TOC concentration of PW can be more than seven times higher peaking at 49,777 mg $L^{-1}$when the BSR is increased from 5 wt.% to 25 wt.% at 220 °C. The suppression of TOC in the liquid phase is important to ease the environmental challenges related to the valorization of PWs. These experimental and statistical results suggest that a trade-off should be made between the solid biofuel yield and quality of process water.

The catalyst-to-suspension ratio is found to be a significant independent variable (p<0.05) in the cases of volatile matter (CSR (L): F = 31.22, p = 0.031) and total organic carbon (CSR (L): F = 169.56, p = 0.006) contents. An upper extremum is identified in the case of FC content in function of the process temperature and CSR (Fig. 2e). The results show that the fixed carbon content can be increased from 9.91 wt.% (T = 180 °C, BSR = 15 wt.%, CSR = 0 wt.%) up to 24.63 wt.% (T = 200 °C, BSR = 25 wt.%, CSR = 7 wt.%). The utilization of acetic acid catalyst improves the fuel properties of HCs, but it also elevates the TOC concentration of the co-produced liquid phase (Fig. 2d). The highest increment (49,977 mg $L^{-1}$) was experienced when the CSR was raised to 10 wt.% at 220 °C and 5 wt.% BSR.

### 3.2. Efficiency of hydrochar production

Improving the conversion of high moisture containing biomass is a key factor to maintain moderate resource management and low greenhouse gas footprint during the hydrothermal treatment. The thermochemical process efficiency of acid catalyzed hydrothermal carbonization was investigated based on performance indicators, i.e., the net energy ratio, energy-, and fixed carbon recovery efficiencies, and heating value.

The results show that the hydrothermal reaction parameters have decisive role in controlling and raising thermochemical conversion efficiencies (Fig. 3). It is obtained that the hydrothermal reaction temperature has an adverse impact on the net energy ratio and energy recovery efficiency. As it is illustrated in Fig. 3a raising temperature from 180 °C to 220 °C reduces the values of NER and $\eta_{ER}$ by 52.5% and 42.1%, respectively. These results suggest that decreasing hydrochar yield has higher negative impact on the energy recovery than the achieved enhanced coalification degree and better combustion properties have in function of the increasing HTC temperature levels. It is obtained that the higher heating value of the solid biofuel and fixed carbon recovery efficiency can be described with curves having maximum points at 19.9 MJ $kg^{-1}$and 69.9% using constant 8 wt.% biomass-to-water ratio; 205°C and 185°C, respectively.

Fig. 3b shows that the biomass-to-suspension ratio has a key role in maintaining high biomass transformation efficiency. The net energy ratio of the catalytic hydrothermal process can be increased by approx. 8-times raising BSR from 5 to 25 wt.%. Simultaneously, the energy-, and fixed carbon recovery efficiencies can be boosted by 43.9% and 46.3%, respectively. However, it is also found that higher biomass-to-suspension levels do not advance the calorific value of solid biofuel samples.

The effects of catalyst-to-suspension ratio on process efficiency indicators are illustrated in Fig. 3c. The utilization of acetic acid catalyst improves fixed carbon recovery efficiency by 23.8% compared to noncatalytic HTC. The addition of the homogeneous catalyst implies the same tendency on the net energy ratio and energy recovery efficiency with attaining minimum values at approx. 4 wt.% CSR level. The $NER_{HTC}$ of the hydrothermal process can be increased by 8.8% up to a value of 3.1 by raising the catalyst concentration up to 10 wt.% at 195 °C and 25 wt.% BSR level. The obtained net energy ratio of catalytic hydrothermal carbonization is in line with former studies that examined the noncatalytic hydrothermal valorization of high moisture containing yard waste (1.4<NER<5.1) [61] and sewage sludge (1.6 < NER < 2.9) [62].

### 3.3. Ex-ante environmental assessment of renewable hydrochar co-firing

The life cycle impacts of hydrochar and coal co-firing were screened

**Table 2**
Life cycle inventory. Functional unit: 1 kWh of produced electricity.

| Process/ Parameters | Units | cHTC | HTC | Data types | Source (s) |
|---|---|---|---|---|---|
| *Chemicals production* | | | | | |
| Energy need of urea production | kWh | 2.39E+00 | 1.86E+00 | Literature based | [50] |
| Energy need of diammonium phoshate production | kWh | 4.84E−01 | 3.77E−01 | Literature based | [59] |
| Energy need of aluminum sulfate production | kWh | 1.46E−04 | 1.14E−04 | Ecoinvent v3.4 | [58] |
| Energy need of acetic acid production | kWh | 6.27E+00 | - | Ecoinvent v3.4 | [58] |
| *Biomass cultivation* | | | | | |
| Mass of urea for Cv cultivation | kg | 3.30E−01 | 2.57E−01 | Literature based | [50] |
| Mass of diammonium phosphate for Cv cultivation | kg | 1.20E−01 | 9.37E−02 | Literature based | [59] |
| Mass of $CO_2$ for Cv cultivation | kg | 3.62E+00 | 2.82E+00 | Literature based | [47] |
| Energy need of paddlewheel | kWh | 1.99E+00 | 1.55E+00 | Literature based | [52] |
| *Biomass harvesting* | | | | | |
| Mass of 0.05 wt. % Cv suspension | kg | 4.36E+03 | 3.39E+03 | Literature based | [53] |
| Mass of aluminum sulfate for Cv harvesting | kg | 4.36E−05 | 3.39E−05 | Literature based | [54] |
| Energy need of clarifier | kWh | 7.01E−04 | 5.46E−04 | Literature based | [42] |
| Energy need of pressure filter | kWh | 5.26E−02 | 4.09E−02 | Literature based | [55] |
| *Biomass transportation* | | | | | |
| Transport of feedstocks to the HTC plant | kgkm | 6.64E+02 | 5.17E+02 | Calculation | Current research |
| *Hydrothermal carbonization* | | | | | |
| Mass of 27 wt.% Cv suspension | kg | 6.64E+00 | 5.17E+00 | Experimental | Current research |
| Mass of acetic acid | kg | 5.74E−01 | - | Experimental | Current research |
| Energy need of mixer | kWh | 1.20E−02 | - | Literature based | [56] |
| Heat requirement of HTC process | kWh | 1.14E+00 | 8.48E−01 | Calculation | Current research |
| *Hydrochar dewatering* | | | | | |
| Mass of hydrochar-process water mixture | kg | 7.21E+00 | 5.17E+00 | Experimental | Current research |
| Energy need of centrifugation | kWh | 1.32E−02 | 1.53E−02 | Literature based | [42] |
| Heat requirement of HC drying | kWh | 3.94E−02 | 4.59E−02 | Calculation | Current research |
| *Hydrochar combustion* | | | | | |
| Mass of dry hydrochar | kg | 6.07E−01 | 7.07E−01 | Calculation | Current research |

on a cradle-to-gate system boundary. As it is illustrated in Fig. 1, distinctive resource management stages were considered for the environmental assessment involving (*i*) the production of chemicals, (*ii*) raw material acquisition, (*iii*) raw material processing, (*iv*) product processing and transport, (*v*) energy conversion and (*vi*) end use. During the impact assessment it is considered that the cHTC co-products, i.e., biogas mixture and process water, are used and recycled in closed emission systems (e.g., as a feedstock in Power-to-Gas energy storage applications or in hydrothermal gasification). As part of raw material acquisition, it was assumed that $CO_2$ is sequestrated from the atmosphere via biofixation. The $CO_2$ uptake rate during the propagation and growing of *Chlorella vulgaris* cells is obtained to be nearly 2-times higher compared to the produced weight of biomass (Eq. 20) offering strong decarbonization potentials for microalgae derived hydrochar blends.

Co-firing compromise between the attainable hydrochar yield and combustion quality was incorporated in the life cycle assessment to support resource management and decision making based on environmental criteria. Comparative life cycle assessment was carried out distinguishing catalytic and noncatalytic hydrothermal processing and co-firing cases, as it is listed in Table 1. Taking into account the investigated efficiency indicators and achievable hydrochar quality, the cHTC and HTC processes are considered to be operated at 195 °C, 25 wt.% BSR, 8 wt.% CSR; and 180 °C, 25 wt.% BSR, 0 wt.% CSR reaction conditions, respectively. Monte Carlo analyses were performed to examine the uncertainty of input and output datasets. The results show no outliers considering the 95% confidence interval and confirm the robustness of the life cycle analyses (Figs. S6–S7).

The energy flow analysis of the catalytic HTC shows that the production of raw chemicals (homogeneous catalyst, fertilizers/substrates for microalgae cultivation, flocculant for harvesting) has the highest utility requirement with a total share of 73.8%. Biomass cultivation in open air system takes the second place with 16.0%. Catalytic hydrothermal carbonization is accounted for only 9.3% of the total utility requirement operating the thermochemical process at ideal reaction conditions. It is also determined that biomass harvesting and hydrochar dewatering have marginal energy demands with an equal share of 0.4%.

The environmental impact assessments show that the application of hydrochar fuel blends is beneficial to reduce the midpoint environmental impacts of coal fired power plants (Table 4). Elevating the hydrochar co-firing ratio is found to be advantageous to mitigate the global warming potential of conventional combined heat power plants using either catalytic or noncatalytic hydrochar blends. It is obtained that negative global warming potential can be achieved in 3 catalytic (A1–A3) and 2 noncatalytic (B1; B2) co-firing cases. The environmental screening of CFR alternatives shows that the attainable advanced energy densification degree of the acetic acid catalyzed hydrothermal carbonization contributes to reach less adverse global warming potentials compared to autocatalytic biomass valorization. The comparative LCA results demonstrate that hydrochars produced via cHTC have lower environmental damages regarding aquatic ecotoxicity, aquatic eutrophication, carcinogens, terrestrial acidification and terrestrial ecotoxicity midpoint categories, compared to noncatalytic HCs at a given CFR value.

The greenhouse gas footprint, electric efficiency and specific electricity production rate of co-firing are illustrated in Fig. 4a. It is obtained that the GHG footprint of pure catalytic hydrochar combustion can be as low as −1.54 kg $CO_{2,eq}kWh^{-1}$in a cradle-to-gate framework, while this value is found to be −1.13 kg $CO_{2,eq}kWh^{-1}$ in the case of noncatalytic hydrothermal carbonization indicating strong decarbonization potentials for hydrochar blends. It is found that GHG emission neutral operation can be reached by applying 43.9% co-firing with catalytic HC blends. The carbon neutral operation is coupled with 27.3% electric efficiency and 187.42 IMPACT 2002+ $\mu$Pt $kWh^{-1}$cumulated environmental damage. Fig. 4a demonstrates that higher blend-to-power efficiency ($X_{CFR} > 30\%$) can be attained with noncatalytic HCs but the co-firing ratio has to be increased to a CFR value of 53.1% in order to

**Table 3**
Design of the experiment for the examination of catalytic hydrothermal carbonization thermochemical process along with measured and calculated results.

| ID | Experimental parameters | | | Proximate analysis | | | HC characteristics | | | | | | PW quality | | Biogas yield |
|---|---|---|---|---|---|---|---|---|---|---|---|---|---|---|---|
| | T (°C) | BSR (wt.%) | CSR (wt.%) | VM (wt. %) | Ash (wt.%) | FC (wt. %) | $Y_{HC}$ (%) | HHV (MJ $kg^{-1}$) | FR (–) | ED (–) | $\eta_{ER}$ (–) | $\eta_{FCR}$ (–) | TOC (mg $L^{-1}$) | pH (–) | $Y_{BC}$ (mol $kg^{-1}$) |
| **1** | 180 | 5 | 0 | 85.69 | 2.12 | 12.19 | 40.83 | 17.65 | 0.142 | 1.035 | 0.283 | 0.278 | 12,140 | 5.59 | 0.51 |
| **2** | 180 | 15 | 10 | 82.10 | 1.53 | 16.37 | 46.72 | 18.57 | 0.199 | 1.089 | 0.444 | 0.556 | 80,270 | 3.59 | 1.40 |
| **3** | 180 | 25 | 5 | 78.75 | 4.39 | 16.85 | 40.74 | 18.20 | 0.214 | 1.068 | 0.220 | 0.289 | 80,070 | 4.05 | 1.59 |
| **4** | 200 | 5 | 10 | 75.92 | 0.32 | 23.76 | 20.58 | 20.23 | 0.313 | 1.187 | 0.164 | 0.274 | 56,700 | 3.40 | 1.71 |
| **5** | 200 | 15 | 5 | 77.37 | 1.32 | 21.31 | 27.34 | 19.59 | 0.275 | 1.149 | 0.437 | 0.676 | 60,300 | 3.93 | 2.04 |
| **6** | 200 | 25 | 0 | 75.12 | 5.11 | 19.76 | 38.02 | 18.66 | 0.263 | 1.094 | 0.266 | 0.401 | 47,950 | 5.47 | 1.84 |
| **7** | 220 | 5 | 5 | 74.82 | 0.92 | 24.26 | 13.84 | 20.23 | 0.324 | 1.187 | 0.485 | 0.826 | 35,050 | 3.70 | 2.20 |
| **8** | 220 | 15 | 0 | 79.09 | 6.66 | 14.25 | 24.33 | 17.32 | 0.180 | 1.016 | 0.475 | 0.555 | 34,040 | 6.46 | 2.54 |
| **9** | 220 | 25 | 10 | 71.55 | 6.50 | 21.95 | 30.26 | 18.87 | 0.307 | 1.107 | 0.335 | 0.554 | 107,100 | 4.01 | 2.44 |
| *Cv* | – | – | – | 82.43 | 5.57 | 11.99 | – | 17.05 | 0.146 | – | – | – | – | – | – |

reach and maintain low-carbon emission operation. Simultaneously, the attributed total impacts can be reduced to 62.54 IMPACT 2002+ $\mu$Pt $kWh^{-1}$that is a major advancement compared to the combustion of hard coal (203.49 IMPACT2002+ $\mu$Pt $kWh^{-1}$).

Fig. 4b demonstrates that the utilization of catalytic and noncatalytic hydrochars imposes different endpoint damages. As it is illustrated in Fig. 4b, higher climate change mitigation potentials can be reached with catalytic based fuel blends. In the case of pure hydrochars, the climate change potential of the catalytic HC is 36% lower compared to the noncatalytic blending component. On the other hand, the damage assessment indicates that higher overall impact reduction can be achieved with the utilization of noncatalytic HCs. The endpoint impact assessment highlights that noncatalytic HC alternatives are preferable over cHTC derived hydrochars in the case of ecosystem quality, human health and resources sub-categories. The midpoint environmental characterization demonstrates that the catalytic hydrochar production implies high respiratory inorganics emission and terrestrial acidification potential (Table 4). These two damage categories have considerable effects on the determined HH and EQ endpoint impacts. Their increased value is the aftereffect of acetic acid utilization including its production, required raw material acquisition and transportation. Using the homogeneous catalyst in the hydrothermal process elevates non-renewable energy and mineral extraction impacts resulting in higher resources endpoint damages. The biofixation of $CO_2$ requires additional chemicals (fertilizers for cultivation, flocculant for harvesting) that also raises the emission of respiratory inorganics. The sustainability analyses show that slightly higher partial damages can be expected on HH in the case of hydrochar co-firing compared to the utilization of hard coal, but HTC scenarios have significant advantage regarding the cumulated environmental impacts and GHG footprint.

The applied energy mix has an important role in pollution prevention and improving process sustainability. Sensitivity analyses are performed to examine the effects of renewable energy mix composition on the GHG footprint sustainability indicator. Fig. 5 presents that changing the ratio of wind turbines and photovoltaic panels in the electricity mix does not pose significant deviations in the final greenhouse footprint value. The sensitivity analysis confirms that higher share of wind energy in the electricity mix is preferred to improve the sustainability of co-firing. It is obtained that the composition of applied renewable energy mix can influence the ideal hydrochar co-firing ratio. 100% catalytic and noncatalytic hydrochar CFR cases show higher sensitivity in function of the renewable energy mix where the A1 and B1 GHG FP values range between −1.28 and −1.54 kg $CO_{2,eq}kWh^{-1}$& −0.91 and −1.13 $CO_{2,eq}kWh^{-1}$, respectively. The *ex-ante* sustainability analyses suggest that carbon neutral operation can be reached by applying 73% or higher share of wind energy ratio in the hydrochar producion chain along with 50% cHTC or 62% HTC co-firing values.

## 4. Discussion

The hydrothermal valorization of wet biomass is found to be an effective process for synthesizing renewable solid biofuels with adequate stability and similar combustion properties to sub-bituminous coals. The statistical analyses confirm that renewable solid fuel properties, i.e., composition, calorific value, fuel ratio can be upgraded and controlled during catalytic and noncatalytic sub-critical thermochemical conversions by adjusting and selecting ideal process parameters. The achievable flexibility in hydrochar quality widens fuel blending possibilities. The combination of high fixed carbon containing coals and renewable hydrochars with elevated volatile content improves the burning performance of conventional fuel resources which are otherwise difficult to ignite. The hydrothermal process performance indicators highlight that quality differences between catalytic and noncatalytic HCs influence the coal co-firing efficiency, the required amount of blending components and indirectly the anthropogenic pollution. The preliminary examinations show that the utilization of homogeneous acetic acid catalyst has a high influence on the sub-critical process performance, hydrochar-, and process water quality. The sustainability assessments indicate that the application of acetic acid catalyst induces different mid-, and endpoint impacts. The climate change mitigation potential can be significantly improved in the cHTC case, but the catalyst utilization increases the $PM_{2.5,eq}$emission. The overall environmental impacts could be reduced by improving the sustainability of applied utilities and auxiliary chemicals production. These findings call the attention to the need for improving the catalytic hydrothermal conversion, screening the environmental effects of other applicable homogeneous and heterogeneous catalysts in hydrothermal processes and demonstrate the importance of process development based on sustainability indicators.

Recycling of side products is important for neutralizing their environmental effects. The high $CO_2$ content of cHTC biogas could be an excellent substrate for photoautotrophic microalgae cultivation or a feedstock in Power-to-Gas applications because of the lack of toxic compounds (e.g., $SO_x$, $NO_x$, heavy metals) in the gas mixture. cHTC reaction conditions have an important role enabling high-quality solid biofuel upgrading along with the co-production of low TOC containing liquid phase. The hydrothermal gasification process seems to be a suitable thermochemical way for the recycling of high TOC containing process waters and to recover gaseous energy carriers [35]. It was also reported that the application of catalysts in the HTG process can improve the TOC reduction of waste waters produced during the hydrothemal valorisation of microalage [63]. In both co-product cases, closed emission systems can be utilized during the resource management preventing the direct emission of hazardous materials. To acquire more complex understanding and a holistic view on the environmental effects of hydrothermal carbonization-based co-firing, future investigations are needed to evaluate and compare side products utilization alternatives.

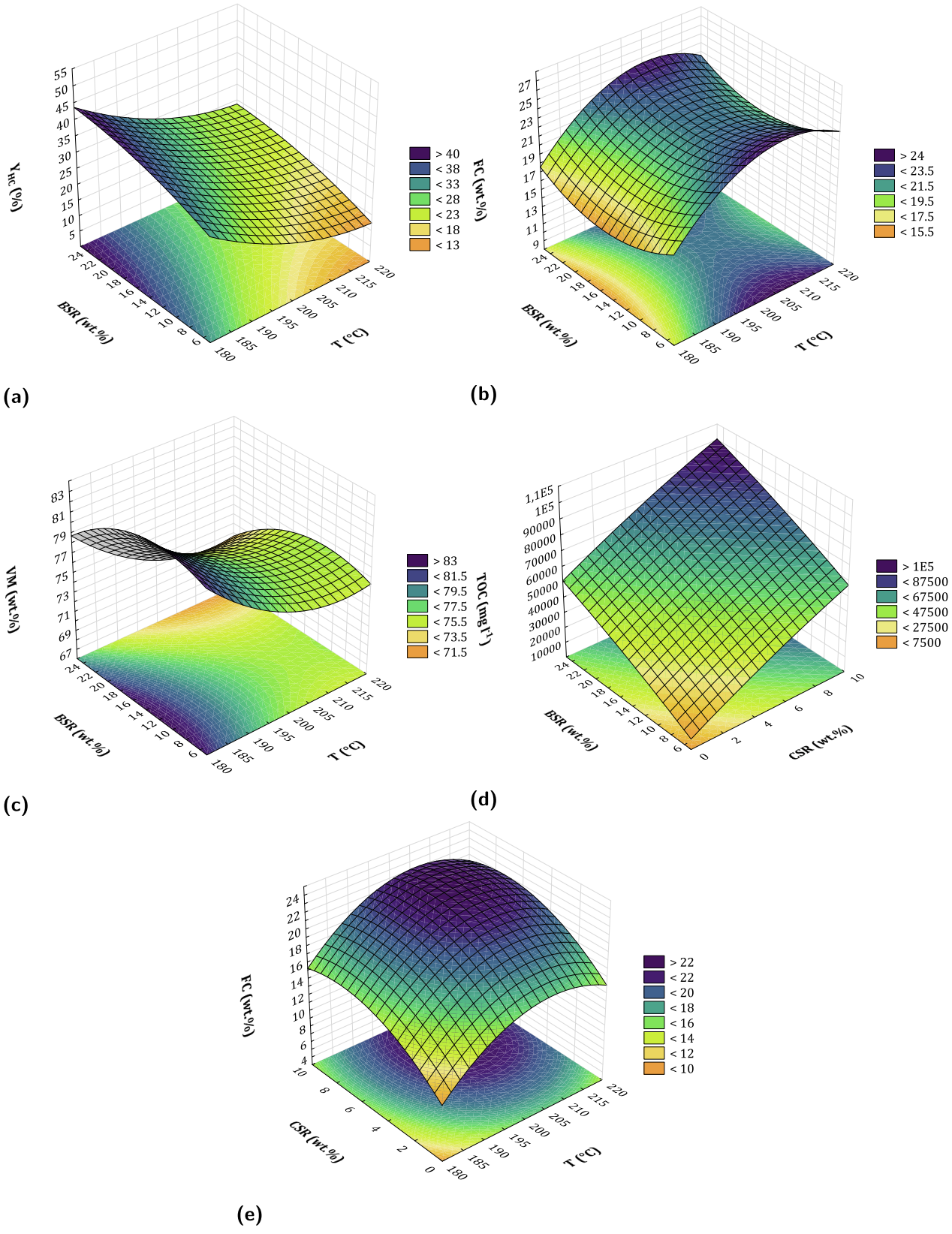


**Fig. 2.** Interactions on 3D plots in the case of catalytic hydrothermal carbonization (cHTC). (a) hydrochar yield in function of temperature and biomass-to-suspension ratio (CSR = 5 wt.%), (b) fixed carbon content of hydrochar in function of temperature and biomass-to-suspension ratio (CSR = 5 wt.%), (c) volatile matter of hydrochar in function of temperature and biomass-to-suspension ratio (CSR = 5 wt.%), (d) total organic carbon content of process water in function of biomass-to-suspension ratio and catalyst-to-suspension ratio (T = 200 °C) and (e) fixed carbon content of hydrochar in function of temperature and catalyst-to-suspension ratio (BSR = 15 wt.%).

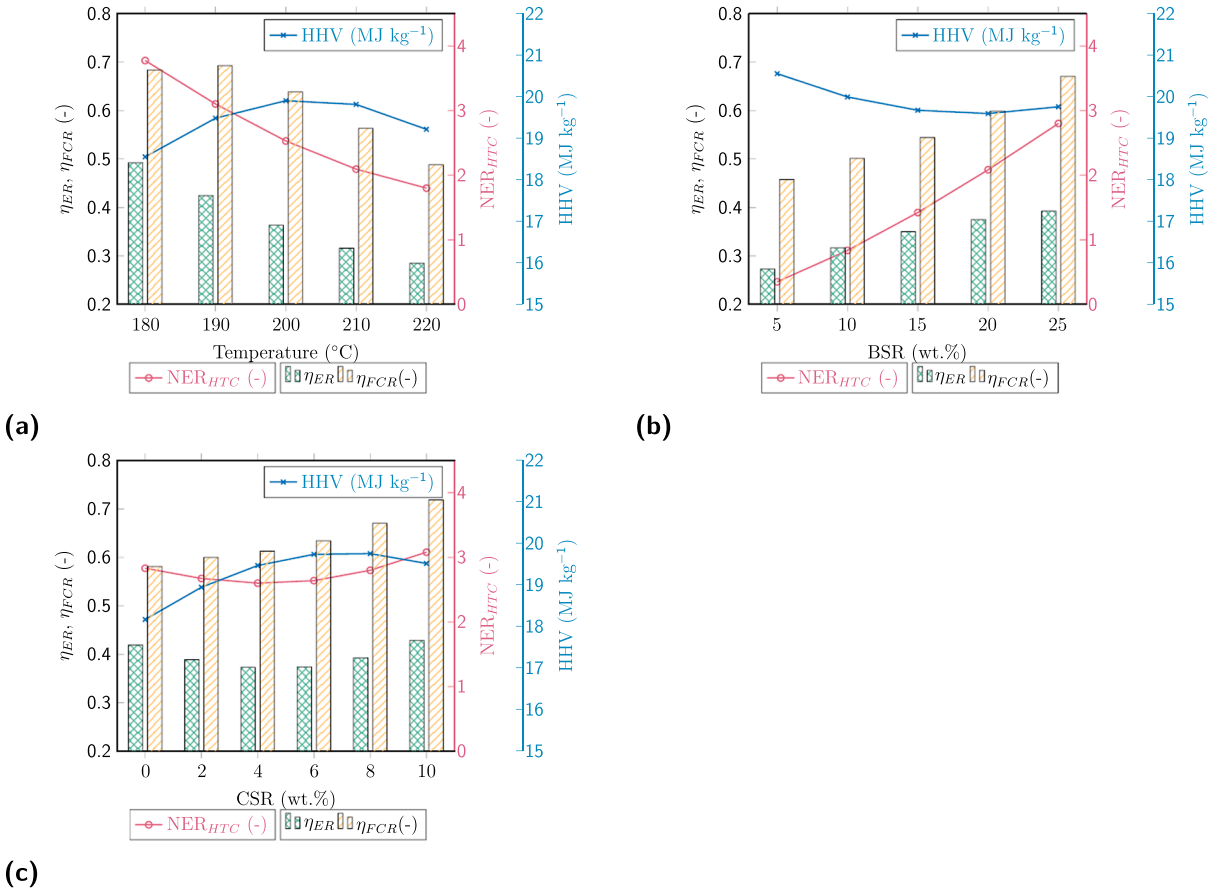


**Fig. 3.** The effects of hydrothermal carbonization process parameters on efficiency indicators. (a) The effects of reaction temperature at 25 wt.% BSR and 8 wt.% CSR; (b) the effects of biomass-to-water ratio at 195 °C and 8 wt.% CSR; and (c) the effects of catalyst-to-suspension ratio at 195 °C, and 25 wt.% BSR.

**Table 4**
Midpoint environmental impacts of hydrochar and coal co-firing alternatives. Functional unit: 1 kWh of produced electricity. CFR: Co-firing ratio.

| Impact category | Unit | A1 (CFR = 100%) 5.66E−03 | A2 (CFR = 75%) 4.21E−03 | A3 (CFR = 50%) 3.06E−03 | A4 (CFR = 25%) 2.12E−03 | B1 (CFR = 100%) 1.20E−03 | B2 (CFR = 75%) 1.25E−03 | B3 (CFR = 50%) 1.29E−03 | B4 (CFR = 25%) 1.32E−03 | C (CFR = 0%) 1.34E−03 |
|---|---|---|---|---|---|---|---|---|---|---|
| Aquatic ecotoxicity | kg TEG water | 1.13E+02 | 7.76E+01 | 4.93E+01 | 2.62E+01 | 2.99E+01 | 2.15E+01 | 1.54E+01 | 1.07E+01 | 7.07E+00 |
| Aquatic eutrophication | kg $PO_4$ P-lim | 5.89E−04 | 4.11E−04 | 2.70E−04 | 1.55E−04 | 2.05E−04 | 1.51E−04 | 1.12E−04 | 8.24E−05 | 5.91E−05 |
| Carcinogens | kg $C_2H_3Cl_{eq}$ | 1.41E−02 | 9.57E−03 | 5.95E−03 | 3.01E−03 | 5.10E−03 | 3.42E−03 | 2.21E−03 | 1.28E−03 | 5.61E−04 |
| Global warming | kg $CO_{2,eq}$ | -1.54E+00 | -6.99E−01 | -2.78E−02 | 5.19E−01 | -1.13E+00 | -3.56E−01 | 2.09E−01 | 6.37E−01 | 9.74E−01 |
| Ionizing radiation | Bq C-14 eq | 1.16E+01 | 7.97E+00 | 5.10E+00 | 2.76E+00 | 1.16E+00 | 1.03E+00 | 9.39E−01 | 8.68E−01 | 8.13E−01 |
| Land occupation | $m^2$org. arable | 1.44E−02 | 1.16E−02 | 9.44E−03 | 7.65E−03 | 5.15E−03 | 5.53E−03 | 5.80E−03 | 6.00E−03 | 6.16E−03 |
| Mineral extraction | MJ surplus | 1.56E−01 | 1.04E−01 | 6.30E−02 | 2.93E−02 | 9.14E−02 | 5.82E−02 | 3.40E−02 | 1.57E−02 | 1.35E−03 |
| Non-carcinogens | kg $C_2H_3Cl_{eq}$ | 2.63E−02 | 1.82E−02 | 1.18E−02 | 6.52E−03 | 1.12E−02 | 7.89E−03 | 5.46E−03 | 3.62E−03 | 2.17E−03 |
| Non-renewable energy | MJ primary | 2.64E+01 | 2.18E+01 | 1.81E+01 | 1.51E+01 | 1.77E+00 | 5.75E+00 | 8.64E+00 | 1.08E+01 | 1.25E+01 |
| Ozone layer depletion | kg CFC-11 eq | 2.78E−07 | 1.86E−07 | 1.13E−07 | 5.28E−08 | 1.79E−08 | 1.25E−08 | 8.51E−09 | 5.51E−09 | 3.17E−09 |
| Respiratory inorganics | kg $PM_{2.5,eq}$ | 1.12E−03 | 8.12E−04 | 5.66E−04 | 3.66E−04 | 2.74E−04 | 2.46E−04 | 2.26E−04 | 2.11E−04 | 1.99E−04 |
| Respiratory organics | kg $C_2H_{4,eq}$ | 6.71E−04 | 4.53E−04 | 2.79E−04 | 1.38E−04 | 8.18E−05 | 5.92E−05 | 4.27E−05 | 3.02E−05 | 2.05E−05 |
| Terrestrial acid/ nutri | kg $SO_{2,eq}$ | 1.62E−02 | 1.23E−02 | 9.20E−03 | 6.68E−03 | 4.02E−03 | 4.23E−03 | 4.38E−03 | 4.49E−03 | 4.58E−03 |
| Terrestrial ecotoxicity | kg TEG soil | 3.06E+01 | 2.10E+01 | 1.32E+01 | 6.94E+00 | 9.82E+00 | 6.83E+00 | 4.66E+00 | 3.01E+00 | 1.71E+00 |

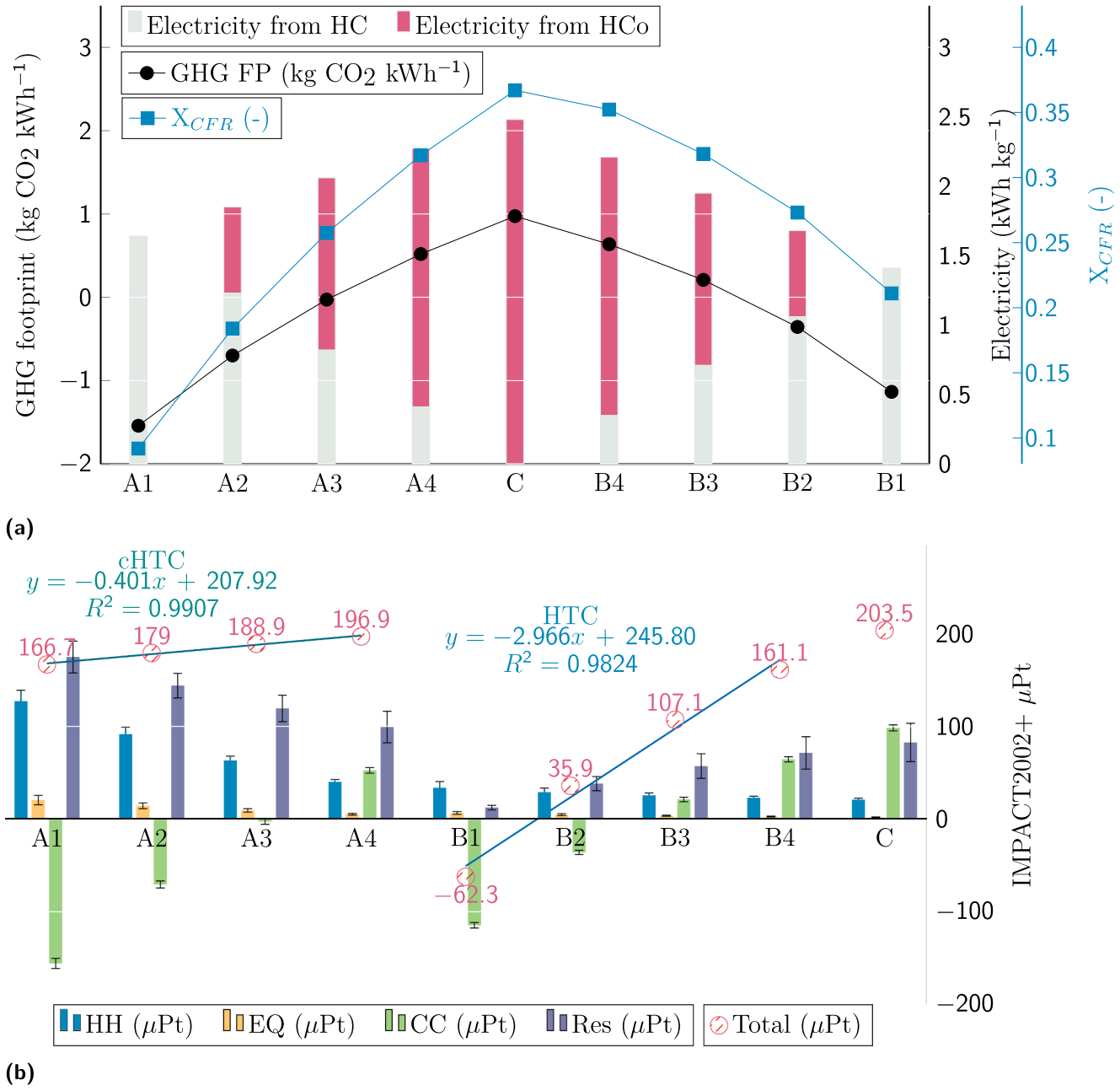


**Fig. 4.** Results of *ex-ante* multi-perspective impact assessment. (a) GHG footprint and overall electric efficiency of HC and HCo co-firing alternatives, (b) Endpoint environmental impacts of hydrochar and coal co-firing alternatives. HH: Human Health, EQ: Ecosystem Quality, CC: Climate Change, Res: Resources, FP: footprint, y = IMPACT2002 + Pt (μPt), x = CFR (%).

The partial substitution of conventional fuels with alternative energy carriers should ensure *(i)* to maintain adequate electricity generation and to *(ii)* meet decarbonization targets. Microalgae-based hydrochars are found to be effective fuel blending components that (1) improve the combustion performance, (2) are characterized by higher stability compared to raw biomass and (3) offers low-carbon transition potentials for fossil-based power plants. The *ex-ante* impact assessment suggests that hydrochar co-firing is an attractive bypass solution allowing to improve the environmental bottlenecks of coal fired power plants where critical focus should be placed on the further development of catalytic hydrothermal valorization and recycling possibilities of side products.

## 5. Conclusions

To improve the sustainability, the efficient production of high-quality biomass-based solid blending components synthesized by catalytic hydrothermal carbonization for coal co-firing is studied. The utilization of acetic acid homogeneous catalyst is found to be beneficial to (1) upgrade the combustion properties of hydrochars, to (2) improve the conversion of dilute *Chlorella vulgaris* microalgae suspension and to (3) decrease the effective co-firing ratio in power plants. The environmental screening highlights that the greenhouse gas footprint of conventional coal fired power plants can be significantly reduced by putting into use renewable hydrochar blends. It is determined that enhanced greenhouse gas emission reduction can be reached by applying 43.9% and 53.1% co-firing ratios in the cases of hydrochars derived from catalyzed and noncatalyzed hydrothermal carbonization processes. The results indicate that the partial substitution of coal with solid hydrothermal biofuels saves natural resources and delivers efficient power generation resulting in low-carbon and sustainable energy generation alternative.

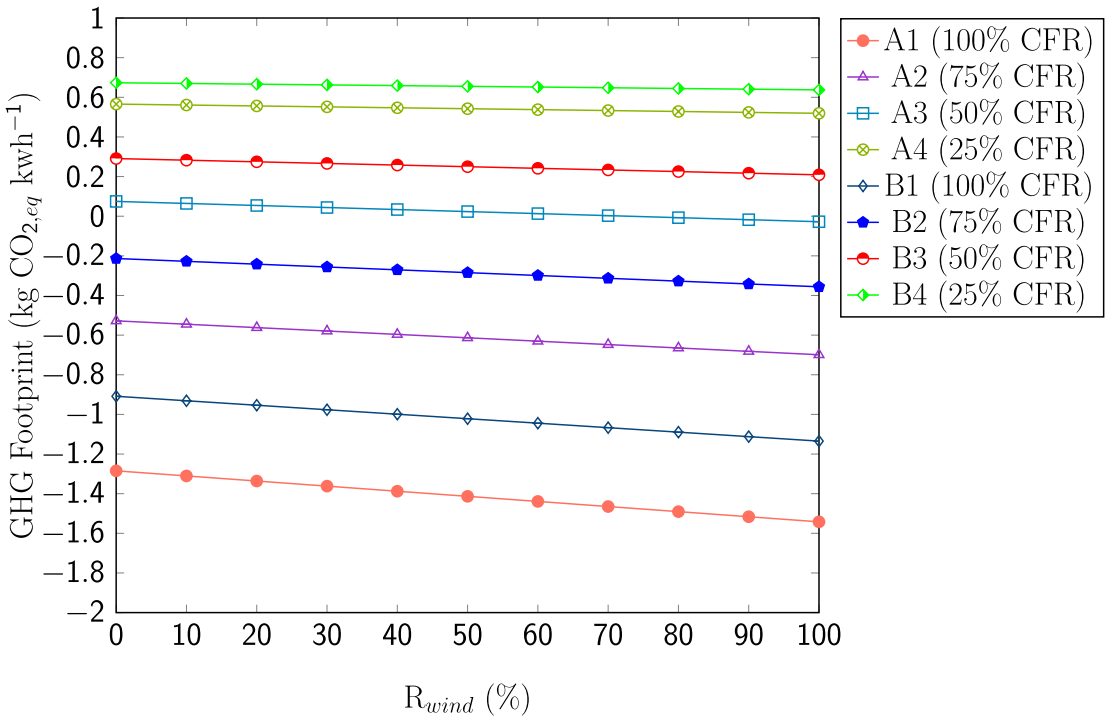


**Fig. 5.** The results of sensitivity analysis for catalytic (A1–A4) and non catalytic (B1–B4) hydrochar co-firing cases. The effects of renewable energy mix composition (wind and solar) on greenhouse gas footprint. $R_{wind}$is the share of wind energy (%) in the applied energy mix.

## CRediT authorship contribution statement

**Greta Sztancs:** Investigation, Conceptualization, Formal analysis, Visualization, Writing - original draft. **Attila Kovacs:** Investigation, Formal analysis. **Andras Jozsef Toth:** Funding acquisition, Data curation. **Peter Mizsey:** Funding acquisition, Methodology. **Pieter Billen:** Writing - review & editing, Methodology. **Daniel Fozer:** Writing - review & editing, Conceptualization, Formal analysis, Visualization, Supervision.

## Declaration of Competing Interest

The authors declare that they have no known competing financial interests or personal relationships that could have appeared to influence the work reported in this paper.

## Acknowledgements

This work was supported by the ÚNKP-20–4-II-BME-296 new national excellence program of the ministry for innovation and technology from the source of the national research, development and innovation fund and the NTP-NFTÖ-20-B-0095 National Talent Program. The authors are grateful for the financial support from the Hungarian National Scientific Research Foundation (OTKA) projects: nr.: 128543 and nr.: 131586. The research reported in this paper and carried out at BME has been supported by the NRDI Fund (TKP2020 NC, Grant No. BME-NC) based on the charter of bolster issued by the NRDI Office under the auspices of the Ministry for Innovation and Technology. The research was supported by the European Union and the Hungarian State, co-financed by the European Regional Development Fund in the framework of the GINOP-2.3.4–15-2016–00004 project aimed to promote the cooperation between the higher education and the industry.

## Appendix A. Supplementary data

Supplementary data associated with this article can be found, in the online version, at https://doi.org/10.1016/j.fuel.2021.120927.

## References

[1] Shukla P, Skea J, Slade R, van Diemen R, Haughey E, Malley J, et al. Climate Change and Land: an IPCC special report on climate change, desertification, land degradation, sustainable land management, food security, and greenhouse gas fluxes in terrestrial ecosystems, techreport. In: Intergovernmental Panel on Climate Change (IPCC) (2019).

[2] Choi YY, Patel AK, Hong ME, Chang WS, Sim SJ. Microalgae Bioenergy with Carbon Capture and Storage (BECCS): An emerging sustainable bioprocess for reduced CO2 emission and biofuel production. Bioresour Technol Rep 2019;7:100270. https://doi.org/10.1016/j.biteb.2019.100270.

[3] Khan MI, Shin JH, Kim JD. The promising future of microalgae: current status, challenges, and optimization of a sustainable and renewable industry for biofuels, feed, and other products. Microbial Cell Factor 17(36). https://doi.org/10.1186/s12934-018-0879-x.

[4] Khoo KS, Chew KW, Yew GY, Leong WH, Chai YH, Show PL, Chen W-H. Recent advances in downstream processing of microalgae lipid recovery for biofuel production. Bioresour Technol 2020;304:122996. https://doi.org/10.1016/j.biortech.2020.122996.

[5] Tang DYY, Khoo KS, Chew KW, Tao Y, Ho S-H, Show PL. Potential utilization of bioproducts from microalgae for the quality enhancement of natural products. Bioresour Technol 2020;304:122997. https://doi.org/10.1016/j.biortech.2020.122997.

[6] Qian L, Wang S, Savage PE. Fast and isothermal hydrothermal liquefaction of sludge at different severities: Reaction products, pathways, and kinetics. Appl Energy 2020;260:114312. https://doi.org/10.1016/j.apenergy.2019.114312.

[7] Kumar M, Oyedun AO, Kumar A. A review on the current status of various hydrothermal technologies on biomass feedstock. Renew Sustain Energy Rev 2018;81:1742–70. https://doi.org/10.1016/j.rser.2017.05.270.

[8] Yang Y, Campana PE, Yan J. Potential of unsubsidized distributed solar PV to replace coal-fired power plants, and profits classification in Chinese cities. Renew Sustain Energy Rev 2020;131:109967. https://doi.org/10.1016/j.rser.2020.109967.

[9] Maamoun N, Kennedy R, Jin X, Urpelainen J. Identifying coal-fired power plants for early retirement. Renew Sustain Energy Rev 2020;126:109833. https://doi.org/10.1016/j.rser.2020.109833.

[10] Yuan Y, Qu Q, Chen L, Wu M. Modeling and optimization of coal blending and coking costs using coal petrography. Inf Sci 2020;522:49–68. https://doi.org/10.1016/j.ins.2020.02.072.

[11] Nawaz Z, Ali U. Techno-economic evaluation of different operating scenarios for indigenous and imported coal blends and biomass co-firing on supercritical coal fired power plant performance. Energy 2020;212:118721. https://doi.org/10.1016/j.energy.2020.118721.

[12] Ozonoh M, Oboirien B, Daramola M. Optimization of process variables during torrefaction of coal/biomass/waste tyre blends: Application of artificial neural network & response surface methodology. Biomass Bioenergy 2020;143:105808. https://doi.org/10.1016/j.biombioe.2020.105808.
[13] Chowdhury MSR, Azad A, Karim MR, Naser J, Bhuiyan AA. Reduction of GHG emissions by utilizing biomass co-firing in a swirl-stabilized furnace. Renewable Energy 2019;143:1201–9. https://doi.org/10.1016/j.renene.2019.05.103.
[14] Sharma HB, Sarmah AK, Dubey B. Hydrothermal carbonization of renewable waste biomass for solid biofuel production: A discussion on process mechanism, the influence of process parameters, environmental performance and fuel properties of hydrochar. Renew Sustain Energy Rev 2020;123:109761. https://doi.org/10.1016/j.rser.2020.109761.
[15] Wang W, Wen C, Li C, Wang M, Li X, Zhou Y, Gong X. Emission reduction of particulate matter from the combustion of biochar via thermal pre-treatment of torrefaction, slow pyrolysis or hydrothermal carbonisation and its co-combustion with pulverized coal. Fuel 2019;240:278–88. https://doi.org/10.1016/j.fuel.2018.11.117.
[16] Aviso K, Sy C, Tan R, Ubando A. Fuzzy optimization of carbon management networks based on direct and indirect biomass co-firing. Renew Sustain Energy Rev 2020;132:110035. https://doi.org/10.1016/j.rser.2020.110035.
[17] Yang B, Wei Y-M, Hou Y, Li H, Wang P. Life cycle environmental impact assessment of fuel mix-based biomass co-firing plants with CO2 capture and storage. Appl Energy 2019;252:113483. https://doi.org/10.1016/j.apenergy.2019.113483.
[18] Zhang N, Wang G, Zhang J, Ning X, Li Y, Liang W, Wang C. Study on co-combustion characteristics of hydrochar and anthracite coal. J Energy Inst 2020;93(3):1125–37. https://doi.org/10.1016/j.joei.2019.10.006.
[19] Sztancs G, Juhasz L, Nagy BJ, Nemeth A, Selim A, Andre A, Toth AJ, Mizsey P, Fozer D. Co-Hydrothermal gasification of Chlorella vulgaris and hydrochar: The effects of waste-to-solid biofuel production and blending concentration on biogas generation. Bioresour Technol 2020;302:122793. https://doi.org/10.1016/j.biortech.2020.122793.
[20] Shen Y. A review on hydrothermal carbonization of biomass and plastic wastes to energy products. Biomass Bioenergy 2020;134:105479. https://doi.org/10.1016/j.biombioe.2020.105479.
[21] Huang C-W, Li Y-H, Xiao K-L, Lasek J. Cofiring characteristics of coal blended with torrefied Miscanthus biochar optimized with three Taguchi indexes. Energy 2019;172:566–79. https://doi.org/10.1016/j.energy.2019.01.168.
[22] Khan TA, Saud AS, Jamari SS, Rahim MHA, Park J-W, Kim H-J. Hydrothermal carbonization of lignocellulosic biomass for carbon rich material preparation: A review. Biomass Bioenergy 2019;130:105384. https://doi.org/10.1016/j.biombioe.2019.105384.
[23] Sermyagina E, Saari J, Kaikko J, Vakkilainen E. Hydrothermal carbonization of coniferous biomass: Effect of process parameters on mass and energy yields. J Anal Appl Pyrol 2015;113:551–6. https://doi.org/10.1016/j.jaap.2015.03.012.
[24] Wang L, Chang Y, Li A. Hydrothermal carbonization for energy-efficient processing of sewage sludge: A review. Renew Sustain Energy Rev 2019;108:423–40. https://doi.org/10.1016/j.rser.2019.04.011.
[25] Zhao X, Stökle K, Becker GC, Zimmermann M, Kruse A. Hydrothermal carbonization of Spirulina platensis and Chlorella vulgaris combined with protein isolation and struvite production. Bioresource Technology Reports 2019;6:159–67. https://doi.org/10.1016/j.biteb.2019.01.006.
[26] Zhang Z, Zhao Y, Wang T. Spirulina hydrothermal carbonization: Effect on hydrochar properties and sulfur transformation. Bioresour Technol 2020;306:123148. https://doi.org/10.1016/j.biortech.2020.123148.
[27] Wang T, Zhai Y, Zhu Y, Li C, Zeng G. A review of the hydrothermal carbonization of biomass waste for hydrochar formation: Process conditions, fundamentals, and physicochemical properties. Renew Sustain Energy Rev 2018;90:223–47. https://doi.org/10.1016/j.rser.2018.03.071.
[28] Nizamuddin S, Baloch HA, Griffin G, Mubarak N, Bhutto AW, Abro R, Mazari SA, Ali BS. An overview of effect of process parameters on hydrothermal carbonization of biomass. Renew Sustain Energy Rev 2017;73:1289–99. https://doi.org/10.1016/j.rser.2016.12.122.
[29] Jain A, Balasubramanian R, Srinivasan M. Hydrothermal conversion of biomass waste to activated carbon with high porosity: A review. Chem Eng J 2016;283:789–805. https://doi.org/10.1016/j.cej.2015.08.014.
[30] García-Bordejé E, Pires E, Fraile JM. Parametric study of the hydrothermal carbonization of cellulose and effect of acidic conditions. Carbon 2017;123:421–32. https://doi.org/10.1016/j.carbon.2017.07.085.
[31] Wang T, Zhai Y, Zhu Y, Peng C, Xu B, Wang T, Li C, Zeng G. Acetic Acid and Sodium Hydroxide-Aided Hydrothermal Carbonization of Woody Biomass for Enhanced Pelletization and Fuel Properties. Energy Fuels 2017;31(11):12200–8. https://doi.org/10.1021/acs.energyfuels.7b01881.
[32] Nunes RS, Tudino TC, Vieira LM, Mandelli D, Carvalho WA. Rational production of highly acidic sulfonated carbons from kraft lignins employing a fractionation process combined with acid-assisted hydrothermal carbonization. Bioresour Technol 2020;303:122882. https://doi.org/10.1016/j.biortech.2020.122882.
[33] Benavente V, Fullana A, Berge ND. Life cycle analysis of hydrothermal carbonization of olive mill waste: Comparison with current management approaches. J Clean Prod 2017;142:2637–48. https://doi.org/10.1016/j.jclepro.2016.11.013.
[34] Tradler SB, Mayr S, Himmelsbach M, Priewasser R, Baumgartner W, Stadler AT. Hydrothermal carbonization as an all-inclusive process for food-waste conversion. Bioresour Technol Rep 2018;2:77–83. https://doi.org/10.1016/j.biteb.2018.04.009.
[35] Watson J, Wang T, Si B, Chen W-T, Aierzhati A, Zhang Y. Valorization of hydrothermal liquefaction aqueous phase: pathways towards commercial viability. Prog Energy Combust Sci 2020;77:100819. https://doi.org/10.1016/j.pecs.2019.100819.
[36] Owsianiak M, Ryberg MW, Renz M, Hitzl M, Hauschild MZ. Environmental Performance of Hydrothermal Carbonization of Four Wet Biomass Waste Streams at Industry-Relevant Scales. ACS Sustain Chem Eng 2016;4(12):6783–91. https://doi.org/10.1021/acssuschemeng.6b01732.
[37] Reiomann D, Thrän D., Bezama A. Hydrothermal processes as treatment paths for biogenic residues in Germany: A review of the technology, sustainability and legal aspects. J Clean Prod 2018;172:239–252. https://doi.org/10.1016/j.jclepro.2017.10.151.
[38] Tibco Software Inc., Tibco statistica 13.4.0, accessed 31.01.2021 (2020). URL: https://docs.tibco.com/products/tibco-statistica-13-4-0.
[39] Parikh J, Channiwala S, Ghosal G. A correlation for calculating HHV from proximate analysis of solid fuels. Fuel 2005;84(5):487–94. https://doi.org/10.1016/j.fuel.2004.10.010.
[40] Leng L, Huang H, Li H, Li J, Zhou W. Biochar stability assessment methods: A review. Sci Total Environ 2019;647:210–22. https://doi.org/10.1016/j.scitotenv.2018.07.402.
[41] Sahu S, Sarkar P, Chakraborty N, Adak A. Thermogravimetric assessment of combustion characteristics of blends of a coal with different biomass chars. Fuel Process Technol 2010;91(3):369–78. https://doi.org/10.1016/j.fuproc.2009.12.001.
[42] Rogers JN, Rosenberg JN, Guzman BJ, Oh VH, Mimbela LE, Ghassemi A, Betenbaugh MJ, Oyler GA, Donohue MD. A critical analysis of paddlewheel-driven raceway ponds for algal biofuel production at commercial scales. Algal Res 2014;4:76–88. https://doi.org/10.1016/j.algal.2013.11.007.
[43] Berk Z. Food Process Engineering and Technology. Elsevier Academic Press; 2009. https://doi.org/10.1016/B978-0-12-373660-4.X0001-4.
[44] United States Envrionmental Protection Agency (EPA), Combined Heat and Power (CHP) Partnership: CHP Benefits, accessed 31.01.2021 (2020). URL: https://www.epa.gov/chp/chp-benefits.
[45] WINGAS, Greenhouse gas emission figures for fossil fuels and power station scenarios in Germany, accessed 31.01.2021 (2014). URL: https://www.wingas.com/en/media-library/studies/study-greenhouse-gas-emission-figures-for-fossil-fuels-and-power-station-scenarios-in-germany.html.
[46] Slater CS, Savelski MJ, Kostetskyy P, Johnson M. Shear-enhanced microfiltration of microalgae in a vibrating membrane module. Clean Technol Environ Pol 2015;17:1743–55. https://doi.org/10.1007/s10098-015-0907-z.
[47] Pate R, Klise G, Wu B. Resource demand implications for US algae biofuels production scale-up. Appl Energy 2011;88(10):3377–88. https://doi.org/10.1016/j.apenergy.2011.04.023.
[48] Dassey AJ, Hall SG, Theegala CS. An analysis of energy consumption for algal biodiesel production: Comparing the literature with current estimates. Algal Res 2014;4:89–95. https://doi.org/10.1016/j.algal.2013.12.006.
[49] Parikh J, Channiwala S, Ghosal G. A correlation for calculating elemental composition from proximate analysis of biomass materials. Fuel 2007;86(12):1710–9. https://doi.org/10.1016/j.fuel.2006.12.029.
[50] Johnson MC, Palou-Rivera I, Frank ED. Energy consumption during the manufacture of nutrients for algae cultivation. Algal Res 2013;2(4):426–36. https://doi.org/10.1016/j.algal.2013.08.003.
[51] Fozer D, Valentinyi N, Racz L, Mizsey P. Evaluation of microalgae-based biorefinery alternatives. Clean Technol Environ Pol 2017;19:501–15. https://doi.org/10.1007/s10098-016-1242-8.
[52] Sompech K, Chisti Y, Srinophakun T. Design of raceway ponds for producing microalgae. Biofuels 2012;3(4):387–97. https://doi.org/10.4155/bfs.12.39.
[53] Surendhiran D, Vijay M. Study on Flocculation Efficiency for Harvesting Nannochloropsis oculata for Biodiesel Production. Int J ChemTech Res 2013;5(4):1761–9.
[54] Dong C, Chen W, Liu C. Flocculation of algal cells by amphoteric chitosan-based flocculant. Bioresour Technol 2014;170:239–47. https://doi.org/10.1016/j.biortech.2014.07.108.
[55] Grima EM, Belarbi E-H, Fernández FGA, Medina AR, Chisti Y. Recovery of microalgal biomass and metabolites: process options and economics. Biotechnol Adv 2003;20(7):491–515. https://doi.org/10.1016/S0734-9750(02)00050-2.
[56] Munter R. Comparison of Mass Transfer Efficiency and Energy Consumption in Static Mixers. Ozone: Sci Eng 2010;32(6):399–407. https://doi.org/10.1080/01919512.2010.517492.
[57] PRé Sustainability, Simapro life cycle assessment software, accessed 31.01.2020 (2020). URL: simapro.com/about/.
[58] Ecoinvent, Ecoinvent database v3.4: life cycle inventory database, accessed 31.01.2021 (2020). URL:v34.ecoquery.ecoinvent.org/Details/PDF/214562A8-2093-4303-A1DC-29DF46FFE06E/06590A66-662A-4885-8494-AD0CF410F956.
[59] Sun X, Wang C, Tong Y, Wang W, Wei J. A comparative study of microfiltration and ultrafiltration for algae harvesting. Algal Res 2013;2(4):437–44. https://doi.org/10.1016/j.algal.2013.08.004.
[60] Heidari M, Dutta A, Acharya B, Mahmud S. A review of the current knowledge and challenges of hydrothermal carbonization for biomass conversion. J Energy Inst 2019;92(6):1779–99. https://doi.org/10.1016/j.joei.2018.12.003.
[61] Akbari M, Oyedun AO, Kumar A. Comparative energy and techno-economic analyses of two different configurations for hydrothermal carbonization of yard

waste. Bioresour Technol Rep 2019;7:100210. https://doi.org/10.1016/j.biteb.2019.100210.
[62] Zhao P, Shen Y, Ge S, Yoshikawa K. Energy recycling from sewage sludge by producing solid biofuel with hydrothermal carbonization. Energy Convers Manage 2014;78:815–21. https://doi.org/10.1016/j.enconman.2013.11.026.
[63] Shan Y-Q, Yin L-X, Djandja OS, Wang Z-C, Duan P-G. Supercritical water gasification of waste water produced from hydrothermal liquefaction of microalgae over Ru catalyst for production of H2 rich gas fuel. Fuel 2021;292:120288. https://doi.org/10.1016/j.fuel.2021.120288.